Coordination chemistry of manganese and iron with N,O-donor ligands: oxidation catalysis and magnetochemistry of clusters

Godbole, M.D.

4

Structural Studies of 'Fe(phoxR)' Complexes and Use in Catalytic Oxidations*

Iron complexes of two ligands, HphoxCOOH and HphoxiPr, have been synthesized and characterized by crystal structure analyses. The complexes $(HNEt_3)_2[Fe(phoxCOO)_2](ClO_4)$ and $[Fe(phoxiPr)_3]$ are reported. Reactions of both ligands RS-HphoxCOOH and RS-HphoxiPr with iron(II)/(III) perchlorates result in the formation of iron complexes with pseudo-octahedral geometry around the metal center. The iron complex of RS-HphoxCOOH has a center of symmetry, and the two ligands are bound in a tridentate manner generating a meridional coordination. Both the dianionic ligands on the metal center have the same chirality. The crystal structure of the complex $(HNEt_3)_2[Fe(phoxCOO)_2](ClO_4)$, is the first accurate structural model of the iron complex of a siderophore analog commonly observed in mycobactins. The complex $[Fe(phoxiPr)_3]$ has three didentate ligands bound in a meridional manner to the metal center. .Each metal ion is surrounded by two ligands of the same chirality and one ligand of opposite chirality (ie. RRS or SSR). The complex $(HNEt_3)_2[Fe(phoxCOO)_2](ClO_4)$ shows promising activity in the oxidation of alkanes, such as toluene, ethylbenzene and cumene, while the complex $[Fe(phoxiPr)_3]$ does not show any catalytic activity in alkane oxidations under the conditions tested. The complex $(HNEt_3)_2[Fe(phoxCOO)_2](ClO_4)$ shows reasonable conversion of H_2O_2 to oxidation products.

* This chapter is based on: Godbole, M. D.; Prat, M.; Tanase, S.; Kooijman, H.; Spek, A. L.; Bouwman, E., 2005. *manuscript in preparation.*

4.1 Introduction

Iron-containing biological molecules are known to play an essential role in a series of metabolic transformations. For example, P-450 selectively oxidizes the long aliphatic side chain of cholesterol, while methane monooxygenase (MMO) converts methane to methanol.[1-4] In both cases, an aliphatic C–H bond is oxidized to give an alcohol product that is liable to further transformations. Structural and functional modelling of these enzymes can be achieved through development of small-molecule models. The synthetic and catalytic studies on such compounds can assist in increasing the understanding of biological reaction mechanisms and to develop new and more efficient catalysts for several of these industrially attractive reactions.

Catalytic oxidations by iron(III)-phoxR complexes (R=COOH, *i*Pr, *i*Pr=isopropyl) has been the topic of current research in the present thesis. The phox-based ligands have N,O-donor groups for coordination to the metal center (Figure 4.1). The stability of the ligands has been proposed to be higher than that of similar ligands containing a C=N moiety (salen-type ligands), as the oxazoline ring is more stable towards oxidative attack.

The ligands of the type HphoxR contain a stereogenic carbon center (C4). When the ligand coordinates to a metal, the substituents at the stereogenic carbon are closest to the metal center. These substituents can, therefore, sterically affect the approach of molecules towards the metal center and hence induce selectivity. The ligands of the type *S*-HphoxCOOR (R=H, CH_3) have been studied initially by Black and Wade,[5] in relation with the synthesis of mycobactins and their chelating analogues. Both the racemic (*RS*), as well as the chiral ligands (*R* or *S*) can be synthesized in straightforward synthetic procedures from the corresponding amino alcohols, or derivatives that are commercially available.

In iron-catalyzed catalytic alkane/alkene oxidations carboxylic acids have been

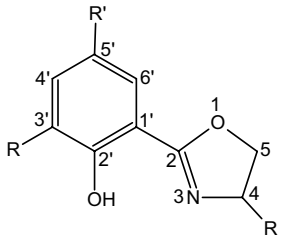

R = COOH (HPhoxCOOH)
R = *i*Pr (Phox*i*Pr)

Figure 4.1: Schematic drawings of the ligands HphoxR.

frequently used as an additive to increase the catalytic activity.[6-9] The mechanism by which these additives increase the activity is unclear yet. Therefore, the HphoxCOOH ligand containing a carboxylate arm that can bind to the metal center has been used in this study. The purpose of the present chapter mainly is to study the coordination behaviour of the ligands (HphoxCOOH and Hphox*i*Pr) with iron and examine their activity in catalytic alkane oxidations and as a model for iron complexes commonly observed in mycobactins. Comparative studies using the ligand Hphox*i*Pr have assisted in elucidating the relation of the activities of the iron complexes with respect to the structures and electronic effects of the ligands.

4.2 Experimental Section

4.2.1 Physical measurements

Elemental analyses were performed with a Perkin-Elmer series II CHNS/O analyzer 2400. Infrared spectra (4000–300 cm^{-1}) were recorded using the reflectance technique on a Perkin–Elmer Paragon 1000 FTIR spectrometer equipped with a Golden Gate ATR device. Diffuse reflectance spectra were obtained on a Perkin-Elmer Lambda 900 spectrophotometer using MgO as a reference. EPR measurements were performed at 77 K using a Jeol Esprit RE-2X spectrometer with a Jeol Esprit 330 ESRE data system. EPR *g* values were determined relative to DPPH as an external ''*g*-marker'' (g = 2.0037). A Johnson Matthey Alfa products Mk1 magnetic susceptibility balance was used to determine the magnetic moments of the powdered complexes at room temperature. Electrospray mass spectra were recorded on a Thermo Finnigan AQA apparatus. A Hewlett Packard 5890 Series II gas chromatograph, equipped with WCOT fused silica column (stationary phase: CP-Was 58 (FFAP) CB) and coupled to a Hewlett Packard 5971 series mass spectrometer with a mass-selective detector was used for analysis of the oxidation experiments.

4.2.2 Syntheses

Caution! Perchlorate salts/complexes are potentially explosive and should be handled with appropriate care. The following abbreviations are used throughout the text: HphoxCOOH = 2-(2'-hydroxyphenyl)-oxazoline-4-carboxylic acid, and Hphox*i*Pr = 2-(2'-hydroxyphenyl)- 4-isopropyloxazoline. All reagents and solvents received from Acros or Sigma-Aldrich, and were used with no attempt to remove water or molecular oxygen. Racemic (*RS*) serine and 2-amino-3-methylbutan-1-ol were ordered from Acros and were

used as received. The ligands HphoxCOOH[5] and Hphox*i*Pr[10] were synthesized using the published procedures.

$(HNEt_3)_4$[Fe(*S*-phoxCOO)$_2$][Fe(*R*-phoxCOO)$_2$]$(ClO_4)_2$: Solid iron(II) perchlorate (0.308 g; 1.21 mmol) was added to a solution of *RS*-HphoxCOOH (0.5 g, 2.41 mmol) in MeOH (15 mL). NEt_3 (1 mL) was added to the solution. The resulting red-purple solution was warmed to 50 °C and stirred for 30 minutes. The solution was filtered and crystals were grown in a few days by layering the MeOH solution with a mixture of THF/pentane (1:1, v/v). The crystalline product was collected by filtration, washed with MeOH and pentane respectively and dried in air. Yield: 55% (0.51 g); UV/VIS (solid): λ_{max}/ nm = 352, 510; IR (diamond): 3016(b), 2659(m), 1607(vs), 1585(vs), 1544(s), 1468(s), 1436(s), 1371(s), 1317(s), 1245(vs), 1162(s), 1089(vs), 929(s), 847(s), 761(vs), 696(s), 622(s), 608(m), 590(m), 565(m), 429(m), 404(m), 390(m), 362(m) cm^{-1}; Anal. Calcd for $(HNEt_3)_2$[Fe(phoxCOO)$_2$](ClO_4), ($C_{32}H_{46}ClFeN_4O_{12}$, FW= 770.03): C, 49.91; H, 6.02; N, 7.28, Found: C, 49.62; H, 6.18; N, 7.32.

***mer*-[Fe(*R,R,S*-phox*i*Pr)$_3$][Fe(*S,S,R*-phox*i*Pr)$_3$]:** Solid iron(III) perchlorate (0.08 g; 0.228 mmol) was added to a solution of *RS*-Hphox*i*Pr (0.1 g, 0.487 mmol) in EtOH (10 mL). 2-3 drops of NEt_3 were also added to the solution. The resulting wine-red solution was warmed to 50 °C and stirred for 3 h. The solution was filtered and crystals were grown in a few days by layering the EtOH solution with Et_2O. The crystalline product was collected by filtration, washed with EtOH and Et_2O respectively and dried in air. Yield: 78% (0.12 g); UV/VIS-NIR (solid): λ_{max}/ nm: 369; 517 IR (diamond): 3550(w, b), 3064(m), 2954(m), 1608(vs), 1542(s), 1469(s), 1441(s), 1379 (m), 1335(s), 1233(s), 1100(s), 1064(s), 959(m), 942(m), 925(m), 850(s), 755(s), 693(m), 664(m), 6034(m), 562(m), 538(m), 387(s) cm^{-1}; Anal. Calcd for [Fe(phox*i*Pr)$_3$], ($C_{36}H_{42}FeN_3O_6$, FW= 668.58): C, 64.67; H, 6.33; N, 6.29, Found: C, 64.44; H, 6.66; N, 6.57.

4.2.3 Catalytic oxidations

In a typical run, 100 equiv of H_2O_2 (30%, 50 μL) were added to an acetonitrile solution (5 mL) containing 5 μmol catalyst and 5 mmol alkane (cyclohexane, cyclooctane or adamantane) at room temperature with a final ratio catalyst : substrate : H_2O_2 = 1 : 1000 : 100. After 180 min of reaction at 30 °C, aliquots were taken from the reaction mixtures and analyzed by GC-MS. At this point, chlorobenzene or 1,2–dibromobenzene was added to the reaction mixtures as internal standard and the samples were analyzed by GC-MS. In all cases

retention times for product peaks were compared with retention time of commercially available products and the identity of the product was checked with GC-MS.

4.2.4 X-ray structure analyses

Pertinent data for the structure determinations are given in Table 4.1. Data were collected at 150 K on a Nonius KappaCCD diffractometer on rotating anode (graphite-monochromated MoKα radiation, λ = 0.71073 Å). The unit-cell parameters were checked for the presence of higher lattice symmetry.[11] The structures were solved with direct methods using SHELXS86.[12] Refinement on F^2 was performed with SHELXL-97.[13] The amine hydrogen atom was located on difference Fourier maps and its coordinates were refined. All other hydrogen atoms were included on calculated positions riding on their carrier atoms. The methyl groups were allowed to rotate along the C—CH_3 bond. One of the ligands of Fe(phox*i*Pr)$_3$ displays disorder, which could be described with a two-site model. The occupancy of the minor component was refined to 0.071(2). Mild distance restraints had to be applied to ensure a reasonable geometry. Neutral atom scattering factors and anomalous dispersion corrections were taken from the International Tables for Crystallography.[14] Validation, geometrical calculations, and illustrations were performed with PLATON.[15]

4.3 Results and Discussion

4.3.1 Description of the Crystal Structures of the Complexes $(HNEt_3)_2[Fe(phoxCOO)_2](ClO_4)$ and [Fe(phox*i*Pr)$_3$]

Crystallographic data for the structures, $(HNEt_3)_2[Fe(phoxCOO)_2](ClO_4)_2$ and [Fe(phox*i*Pr)$_3$] are collected in Table 4.1. Relevant bond distances and angles for the complexes are collected in Table 4.2. PLUTON projections of molecules of the complexes $(HNEt_3)_2[Fe(phoxCOO)_2](ClO_4)$ and [Fe(phox*i*Pr)$_3$] are shown in Figure 4.2 and Figure 4.4 respectively.

In the complex $(HNEt_3)_2[Fe(phoxCOO)_2](ClO_4)_2$, the racemic mixture of the ligand *RS*-phoxCOO is separated to form a diastereomeric/enantiomeric mixture of iron complexes, *mer*-[Fe(*S*-phoxCOO)$_2$]$^-$ and *mer*-[Fe(*R*-phoxCOO)$_2$]$^-$, which are related by an inversion center and therefore present in a 1:1 ratio in the solid state. In Figure 4.2 only the molecule of complex [Fe(*S*-phoxCOO)$_2$]$^-$ is shown. This observation is similar to the chiral separation in the solid state as observed for the manganese complex of the ligand HphoxCOOH (see chapter 3).[16] The asymmetric unit contains half a molecule of [Fe(phoxCOO)]$^-$ located on a two-fold rotation axis, half a perchlorate anion located on a mirror plane, and one molecule of

protonated triethylamine. The phoxCOO ligands are deprotonated at both the acid and the phenol moiety. The iron(III) center has a N_2O_4 coordination sphere with pseudo-octahedral geometry. Both ligands are bound to the iron center in a meridional fashion. The ligands are orthogonal, and coordinate to the metal center with the phenolate oxygen atom, the nitrogen atom of the oxazoline ring, and the carboxylate oxygen atom. The Fe–N distance is 2.0597(15) Å and the Fe–O(phenolate) distance is 1.9188(13) Å. The Fe–O(carboxylate) (2.1010(13) Å) distance is longer than that of Fe–O(phenolate). These distances are very similar to those in the $[Fe(ehpg)]^-$ complexes (H_4ehpg = ethylene-*N*,*N*'-bis((2-hydroxyphenyl)-glycine),[17] but are longer than in the complex $[Fe(hped)]^-$ (H_4hped = *N*,*N*'-bis(2-hydroxyphenyl)ethylenediamine-*N*,*N*'-diacetate).[18]

Hydrogen bonds are donated by the protonated amine molecules to the deprotonated acid moieties of the iron complex. A discrete cluster of the composition $\{2(HNEt_3)\cdot[Fe(phoxCOO)_2]\}^+$ is formed via these hydrogen bonds (Figure 4.3) with a N(51)–H(51)···O(27) distance of 2.773(2) Å.

The arrangement of the phoxCOO ligands in this iron complex is markedly different from the analogous manganese complex, (H_2NEt_2) *fac-cct*-[Mn(*R*-phoxCOO)$_2$],[16] which shows a *fac-cct* arrangement of the ligands around manganese, the complex lacking any center or axis of symmetry. The complex (H_2NEt_2) *fac-cct*-[Mn(*R*-phoxCOO)$_2$] shows strong distortion in the phenol-oxazoline ligand backbone, whereas in the iron complex $(HNEt_3)_2[Fe(phoxCOO)_2](ClO_4)$ the phenol-oxazoline ligand backbone shows a rather small distortion. The dihedral angles between the phenol ring and the oxazoline ring for the two

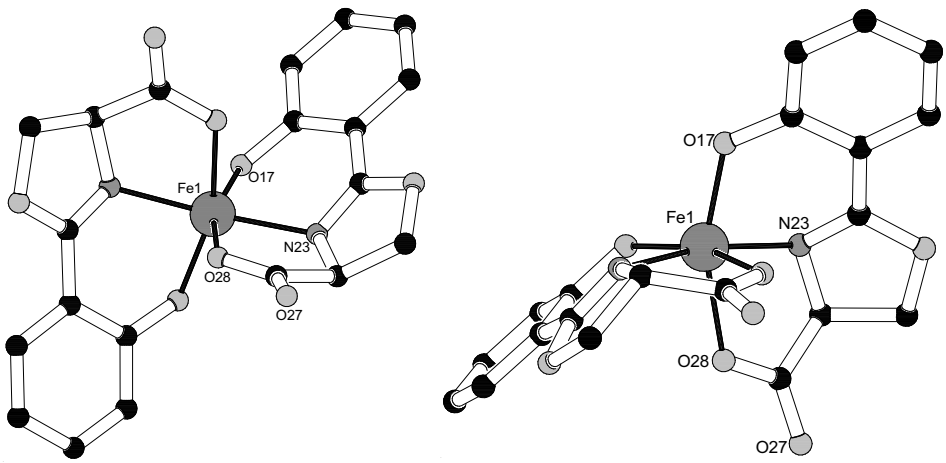

Figure 4.2: PLUTON projections of the molecule of the anionic complex, $(HNEt_3)_4[Fe(S\text{-phoxCOO})_2][Fe(R\text{-phoxCOO})_2](ClO_4)_2$ showing the anionic complex *mer*-$[Fe(S\text{-phoxCOO})_2]^-$. The hydrogen atoms are omitted for clarity.

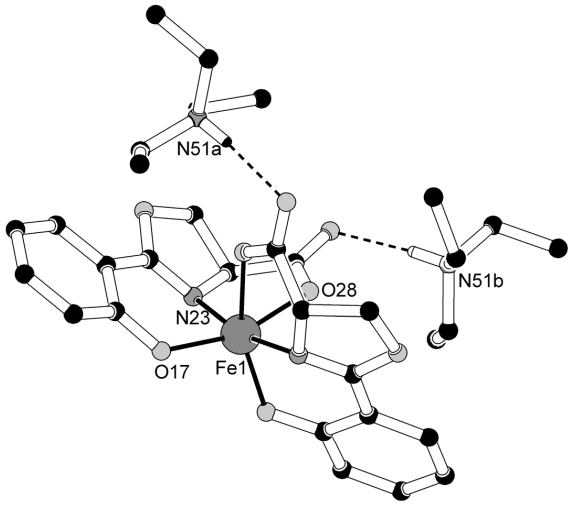

Figure 4.3: A PLUTON projection of hydrogen bonding in the complex $(HNEt_3)_2[Fe(phoxCOO)_2](ClO_4)$. Hydrogen atoms except those participating in hydrogen bonding are omitted for clarity.

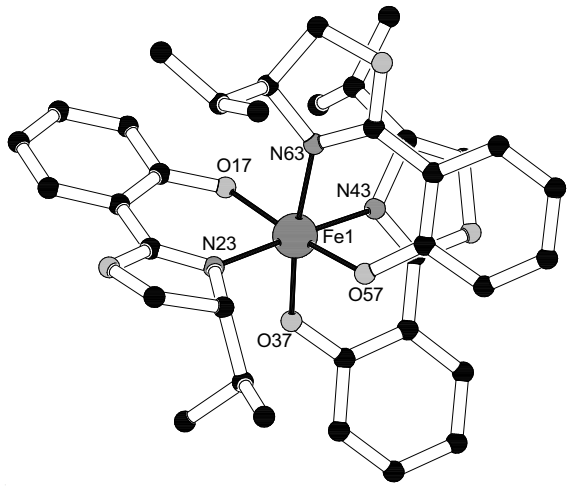

Figure 4.4: PLUTON projection of a molecule of the complex *mer*-[Fe(*R*-phox*i*Pr)$_2$(*S*-phox*i*Pr)][Fe(*S*-phox*i*Pr)$_2$(*R*-phox*i*Pr)] showing a molecule of the complex *mer*-[Fe(*R*-phox*i*Pr)$_2$(*S*-phox*i*Pr)]. Hydrogen atoms are omitted for clarity.

ligands in the iron complex is 7.97(10) as opposed to the dihedral angle of 25.08(16)° and 21.09(13)° in the manganese complex. However, in the iron complex $(HNEt_3)_2[Fe(phoxCOO)_2](ClO_4)$ the phenolate-oxazoline chelate ring (O17–C11–C12–C22–N23) is tilted from the Fe1–O17–N23 plane by 37.26(8)° versus 15.66(14)° and 12.80(12)° in the manganese complex.

Structures similar to the above complex have been reported in literature with other metals in relevance to the coordination chemistry studies on metal complexes of the

Table 4.1: Crystallographic data for $(HNEt_3)_2[Fe(phoxCOO)_2](ClO_4)$ and [Fe(phox*i*Pr)$_3$].

	$(HNEt_3)_2[Fe(phoxCOO)_2](ClO_4)$	**[Fe(phox*i*Pr)$_3$]**
Formula	$C_{32}H_{46}ClFeN_4O_{12}$	$C_{36}H_{42}FeN_3O_6$
Fw, g/mol	770.03	668.58
a, Å	30.166(3)	11.2281(10)
b, Å	19.167(4)	20.947(3)
c, Å	12.7528(10)	15.106(2)
β, deg	-	111.297(10)
V, Å^3	7373.6(18)	3310.2(7)
Z	8	4
space group	Cmca, No: 64,	$P2_1/c$ (No: 14)
crystal system	Orthorhombic	Monoclinic
ρ_{calc}, g/cm^3	1.3873(3)	1.3416(3)
T, K	150	150
μ(MoKα) mm^{-1}	0.546	0.506
total reflns	97220	53882
unique reflns	4330	5999
parameters	237	445
R, *wR*2	0.043, 0.110	0.034, 0.086
S	1.12	1.06

naturally-occurring siderophores (such as ferrithiocin) and their synthetic analogs.[19, 20] The stereochemistry of the above complex is very similar to that of the complex $(HNEt_3)[Cr(dfft)_2]$ (H_2dfft = Desferriferrithiocin).[19] In fact, the present iron complex is the first structurally-characterized analog for an iron-siderophore complex as established in mycobactins, albeit that the thiazoline ring is replaced by an oxazoline ring.[19, 20]

The complex [Fe(phox*i*Pr)$_3$] crystallizes in the centrosymmetric space group $P2_1/c$. The structure of the iron complex in an asymmetric unit is [Fe(phox*i*Pr)$_3$] containing three phox*i*Pr ligands coordinating to the iron center. Two of the ligands are in *R* conformation and third as *S* ([Fe(*RRS* -phoxiPr)$_3$]). Due to the center of symmetry, the complex is also present as [Fe(*SSR*-phoxiPr)$_3$]. The iron(III) center therefore, has a N_3O_3 coordination sphere with pseudo-octahedral geometry. Also in this case, the three ligands are bound to the iron center in the meridional fashion. Two of the three ligands bound to the metal center have the *R* configuration at C4 and the third ligand has the *S* configuration at C4. Thus, the iron complex in this conformation (conformation A) can be depicted as [Fe(*RRS*-phoxiPr)$_3$]. Furthermore, one of the ligands with *R* configuration at C4 displays disorder in the configuration: in 7.1% of the molecules in the unit cell this ligand has the opposite chirality and a different conformation (conformation 'B') (the main conformation is conformation 'A'). Thus, the iron complex in this configuration can be illustrated as [Fe(*SRS*-phox*i*Pr)$_3$] in the conformation B.

Table 4.2: Selected bond angles and distances for complexes $(HNEt_3)_2[Fe(phoxCOO)_2](ClO_4)$ and $[Fe(phox\textit{i}Pr)_3]$.

$(HNEt_3)_2[Fe(phoxCOO)_2](ClO_4)$		**$[Fe(phox\textit{i}Pr)_3]$**	
Fe(1)-O(17)	1.9188(13)	Fe(1)–O(17)	1.9340(13)
Fe(1)–O(28)	2.1010(13)	Fe(1)–O(37)	1.9452(14)
Fe(1)–N(23)	2.0597(15)	Fe(1)–O(57)	1.9643(13)
O(17)–Fe(1)–O(28)	159.30(5)	Fe(1)–N(23)	2.110(3)
O(17)–Fe(1)–N(23)	84.94(6)	Fe(1)–N(43)	2.1602(18)
O(17)–Fe(1)–O(17)b	103.77(5)	Fe(1)–N(63)	2.1485(17)
O(17)–Fe(1)–O(28)b	89.53(5)	O(17)–Fe(1)–O(37)	96.98(6)
O(17)–Fe(1)–N(23)b	102.72(6)	O(17)–Fe(1)–O(57)	171.56(6)
O(28)–Fe(1)–N(23)	76.59(5)	O(17)–Fe(1)–N(23)	85.73(9)
O(28)–Fe(1)–O(28)b	82.63(5)	O(17)–Fe(1)–N(43)	92.68(6)
O(28)–Fe(1)–N(23)b	94.09(5)	O(17)–Fe(1)–N(63)	89.34(6)
N(23)–Fe(1)–N(23)b	167.73(6)	O(37)–Fe(1)–O(57)	91.33(6)
		O(37)–Fe(1)–N(23)	92.04(9)
		O(37)–Fe(1)–N(43)	84.16(6)
		O(37)–Fe(1)–N(63)	172.09(6)
		O(57)–Fe(1)–N(23)	92.53(9)
		O(57)–Fe(1)–N(43)	89.62(6)
		O(57)–Fe(1)–N(63)	82.50(6)
		N(23)–Fe(1)–N(43)	175.68(9)
		N(23)–Fe(1)–N(63)	93.18(9)
		N(43)–Fe(1)–N(63)	90.82(7)

Therefore, the unit cell contains 3.55% molecules as *RSR* in conformation B, 3.55% molecules as *SRS* in conformation B, (total B: 7.1%); 46.45% molecules as *RRS* in conformation A, and 46.45% molecules as *SSR* in conformation A, (total A: 92.9%). The Fe–N distances are significantly longer than the Fe–O(phenolate) distances; the distances are comparable to the usually observed Fe–N and Fe–O distances.[21, 22]

Several Fe(III) complexes containing N_3O_3 coordination sphere have been reported in literature with the ligands 2-(2'-hydroxyphenyl)-oxazoline (Hphox),[21] 2-methylquinolin-8-olate,[23] 1,1,1-tris(2-hydroxybenzylideneamino)-methylpropane,[24] 3(5)-methyl-5(3)-(2-hydroxyphenyl)pyrazole (H_2phpz).[22] Most of these complexes also show a meridional conformation, however, the $[Fe(phox)_3]$ complex has been proposed to be a mixture of meridional and facial conformations, due to the symmetry-related disorder observed in the crystal structure.[21]

4.3.2 Synthetic and Spectroscopic Aspects

The synthesis of the ligands HphoxCOOH and Hphox*i*Pr has been reported previously.[5, 10] Reaction of Fe(II) perchlorate with the racemic ligand *RS*-HphoxCOOH in the

presence of triethylamine, results in the formation of the dark-red, complex $(HNEt_3)_4[Fe(phoxCOO)_2](ClO_4)_2$ which crystallizes as a double salt with $(HNEt_3)(ClO_4)$.

Reaction of racemic ligand, *RS*-Hphox*i*Pr with Fe(III) perchlorate results in the straightforward formation of the ML_3 complex [Fe(phox*i*Pr)$_3$]. Solid-state ligand field spectra of both complexes show bands that are very similar in position. In both complexes, the intense band at around 510-517 nm can be assigned to the phenolate(pπ)→Fe(III)(dπ) LMCT transition,[25] and the band at around 350 nm can be assigned to the phenolate(pπ)→Fe(III)(dσ) charge-transfer transition.[25]

Coordination of the ligand to the metal center is confirmed in both complexes from the shift of the C=N peak in the IR spectrum from around 1690 cm^{-1} in the free ligands to about 1610-1629 cm^{-1} in the metal complexes.[26] In addition, the symmetric and antisymmetric stretching vibrations of the oxazoline ring alkyl protons in both complexes are observed at 3016 and 3093 cm^{-1} in the complexes $(HNEt)_2[Fe(phoxCOO)_2](ClO_4)$ and [Fe(phox*i*Pr)$_3$] respectively.[27] The complex $(HNEt_3)_2[Fe(phoxCOO)_2](ClO_4)$ also shows a strong peak due to the presence of non-coordinating perchlorate counterion at 1089 cm^{-1}.

4.3.3 Catalytic Alkane Oxidations

The catalytic activity of the complexes $(HNEt_3)_2[Fe(phoxCOO)_2](ClO_4)$ and [Fe(phox*i*Pr)$_3$] has been tested in the oxidation of different alkanes (cyclohexane, cyclooctane, adamantane, toluene, ethylbenzene, cumene) with dihydrogen peroxide under ambient conditions. In all cases, a catalyst/substrate/H_2O_2 molar ratio of 1/1000/100 has been employed. The catalytic oxidation of alkanes was carried out by using an excess of substrate

Table 4.3: Alkane oxidations catalyzed by $(HNEt_3)_2[Fe(phoxCOO)_2](ClO_4)$.[a]

Substrate	Product	TON[b]	conversion/based on H_2O_2 (%)
Toluene	Benzaldehyde	3.2	13.3
	Benzyl alcohol	10.1	
Ethylbenzene	acetophenone	8.8	19.8
	R, S-phenylethyl alcohol	11.0	
Cumene	Acetophenone	5.2	13.5
	2-phenyl-2-propanol	6.5	
	α- methyl styrene	1.8	

a: Reaction conditions: Catalyst:Substrate:H_2O_2 = 1:1000:100, 5 ml 1 mM solution of the catalyst (5 μmol) in Acetonitrile.
b: TON = turnover number of the product in mole product per mole catalyst obtained after 180 minutes.

(RH) with respect to the oxidant to make sure that during the entire course of the reaction the concentration of the oxidized substrate (ROH) is substantially lower than that of the substrate in order to minimize oxidation of ROH. A large substrate/H_2O_2 ratio was also expected to minimize decomposition of H_2O_2 (catalase activity). The complex [Fe(phox*i*Pr)$_3$] was found to be inactive in the oxidation of alkanes, whereas $(HNEt_3)_2$[Fe(phoxCOO)$_2$](ClO_4) shows modest catalytic activity in the oxidation of toluene, ethylbenzene and cumene (Table 4.3).

The oxidation of toluene catalyzed by $(HNEt_3)_2$[Fe(phoxCOO)$_2$](ClO_4) gives benzyl alcohol (10.1 TON) as the main product along with a small amount of benzaldehyde (3.2 TON), with a final conversion of 13.3% based on H_2O_2. Slightly higher activity (19.8% conversion based on H_2O_2) was observed in the oxidation of ethylbenzene; acetophenone (8.8 TON) and *R*,*S*-phenethyl alcohol (11 TON) were the main products. Cumene as substrate afforded 2-phenyl-2-propanol (6.5 TON), acetophenone (5.2 TON) and α-methyl-styrene (1.8 TON); a total conversion of 13.5 % based on H_2O_2 was reached in this case. By comparison to literature, the percentage conversion based on 100 equivalents of H_2O_2 in the range of 13-19% is a relatively high conversion of dihydrogen peroxide into the oxidation products. For example the percentage yield in the oxidation of toluene by the complex [Fe(tpaa)](ClO_4)$_2$ (tpaa = tris-[*N*-(2-pyridylmethyl)-2-aminoethyl]amine) is reported to be 18.5 % in total, based on 20 eq H_2O_2 (i.e. 3.7 molecules of H_2O_2 converted to oxidation products).[28]

The absence of catalytic activity in the oxidation of cyclohexane, cyclooctane and adamantane suggest that the complex $(HNEt_3)_2$[Fe(phoxCOO)$_2$](ClO_4) is unable to hydroxylate alkanes with higher C–H bond dissociation energies. The complex in principle is expected to show less activity as any catalytic activity requires the presence of a minimum of one or two open sites for the binding and activation of the oxidant to take place.[29, 30] Despite the hexa-coordination, the complex $(HNEt_3)_2$[Fe(phoxCOO)$_2$](ClO_4) is active in catalytic oxidations. This reactivity suggests that one or two of the ligand donors dissociate before or during catalysis, and points to the possibility that the structure of the original complex might not be conserved during the catalytic activity. Differences in the catalytic ability of the complexes $(HNEt_3)_2$[Fe(phoxCOO)$_2$](ClO_4) and [Fephox*i*Pr)$_3$] could possibly arise from a combination of a few factors. The strain associated with the tridentate binding of the phoxCOO ligand could lead to dissociation of one or more ligand donors, thus opening sites on the metal center for catalysis to take place. In addition, the carboxylate groups on the phoxCOOH ligand are electron-withdrawing as compared to the electron-donating nature of the isopropyl substituent on the phoxiPr ligand.

4.4 Concluding Remarks

The iron complexes of the ligands HphoxCOOH and HphoxiPr exhibit interesting structural preferences owing to the chirality and denticity of the ligands. The iron complex of *RS*-HphoxCOOH is octahedral with a center of symmetry, with two ligands bound in a meridional fashion in a tridentate manner. Both the dianionic ligands have same chirality, and are mutually perpendicular. The arrangement of the phoxCOO ligands in this iron complex is markedly different from the analogous manganese complex, (H_2NEt_2) *fac-cct*-[Mn(*R*-phoxCOO)$_2$].[16] The crystal structure of the complex $(HNEt_3)_2[Fe(phoxCOO)_2](ClO_4)$, is the first accurate structural model of iron complex of a siderophore analog commonly observed in mycobactins. The reaction of the ligand *RS*-Hphox*i*Pr with iron(III) perchlorate results in the formation of a $[FeL_3]$ complex with an octahedral geometry, wherein three didentate ligands are bound with the O atoms in a meridional orientation to the metal center.

The present complexes have been used in catalytic alkane oxidations. The complex $(HNEt_3)_2[Fe(phoxCOO)_2](ClO_4)$ shows modest activity in the oxidations of alkanes, such as toluene, ethylbenzene and cumene, with relatively high conversions of dihydrogen peroxide, while the complex [Fe(phox*i*Pr)$_3$] does not show any catalytic activity in alkane oxidations.

4.5 References

1. Sono, M.; Roach, M. P.; Coulter, E. D.; Dawson, J. H., *Chem. Rev.* 1996, 96, 2841-2887.
2. Costas, M.; Chen, K.; Que, L., *Coord. Chem. Rev.* 2000, 200, 517-544.
3. Abu-Omar, M. M.; Loaiza, A.; Hontzeas, N., *Chem. Rev.* 2005, 105, 2227-2252.
4. Denisov, I. G.; Makris, T. M.; Sligar, S. G.; Schlichting, I., *Chem. Rev.* 2005, 105, 2253-2277.
5. Black, D. S. C.; Wade, M. J., *Aust. J. Chem.* 1972, 25, 1797-1810.
6. White, M. C.; Doyle, A. G.; Jacobsen, E. N., *J. Am. Chem. Soc.* 2001, 123, 7194-7195.
7. Tanase, S.; Foltz, C.; de Gelder, R.; Hage, R.; Bouwman, E.; Reedijk, J. R., *J. Mol. Cat. A* 2005, 225, 161-167.
8. Nizova, G. V.; Krebs, B.; Suss-Fink, G.; Schindler, S.; Westerheide, L.; Cuervo, L. G.; Shul'pin, G. B., *Tetrahedron* 2002, 58, 9231-9237.
9. Fujita, M.; Que, L., *Adv. Synth. Catal.* 2004, 346, 190-194.
10. Bolm, C.; Weickhardt, K.; Zehnder, M.; Ranff, T., *Chem. Berichte* 1991, 124, 1173-1180.
11. Spek, A. L., *J. Appl. Crystallogr.* 1988, 21, 578-579.
12. Sheldrick, G. M. *SHELXS-86: Program for X-Ray structure determination*, University of Göttingen: Göttingen (Germany), 1986.
13. Sheldrick, G. M. *SHELXS-97:Program for crystal structure determination*, University of Göttingen: Göttingen (Germany), 1997.
14. Wilson, A. J. C. (ed.), *International Tables for Crystallography*, Vol. C, Kluwer Academic Publishers: Dordrecht, The Netherlands, 1992.
15. Spek, A. L., *J. Appl. Crystallogr.* 2003, 36, 7-13.
16. Godbole, M. D.; Hotze, A.; Hage, R.; Mills, A. M.; Kooijman, H.; Spek, A. L.; Bouwman, E., *Inorg. Chem. in press* 2005.
17. Bailey, N. A.; Cummins, D.; McKenzie, E. D.; Worthington, J. M., *Inorg. Chim. Acta* 1981, 50, 111-120.
18. Larsen, S. K.; Jenkins, B. G.; Memon, N. G.; Lauffer, R. B., *Inorg. Chem.* 1990, 29, 1147-1152.

19. Hahn, F. E.; McMurry, T. J.; Hugi, A.; Raymond, K. N., *J. Am. Chem. Soc.* 1990, 112, 1854-1860.
20. Langemann, K.; Heineke, D.; Rupprecht, S.; Raymond, K. N., *Inorg. Chem.* 1996, 35, 5663-5673.
21. Kooijman, H.; Spek, A. L.; Hoogenraad, M.; Bouwman, E.; Haasnoot, J. G.; Reedijk, J., *Acta Crystallogr. Sect. C-Cryst. Struct. Commun.* 2002, 58, m390-m392.
22. Tanase, S.; Bouwman, E.; Long, G. J.; Shahin, A. M.; Mills, A. M.; Spek, A. L.; Reedijk, J. R., *Eur. J. Inorg. Chem.* 2004, 4572-4578.
23. Jian, F. F.; Wang, Y.; Lu, L. D.; Yang, X. J.; Wang, X.; Chantrapromma, S.; Fun, H. K.; Razak, I. A., *Acta Crystallogr. Sect. C-Cryst. Struct. Commun.* 2001, 57, 714-716.
24. Reglinski, J.; Patykiewicz, M., *Acta Crystallogr. Sect. E.-Struct Rep. Online* 2002, 58, M543-M544.
25. Gaber, B. P.; Miskowsk.V; Spiro, T. G., *J. Am. Chem. Soc.* 1974, 96, 6868-6873.
26. Lin-Vien, D.; Colthup, N. B.; Fateley, W. G.; Grasselli, J. G., *The Handbook of infrared and Raman characteristic frequencies of organic molecules*. Academic Press Limited, London, 1991; p 200.
27. Socrates, G., *Infrared Characteristic Group Frenquencies*. John Wiley and Sons, Bath, 1980; p 3.
28. Balland, V.; Mathieu, D.; Pons-Y-Moll, N.; Bartoli, J. F.; Banse, F.; Battioni, P.; Girerd, J. F.; Mansuy, D., *J. Mol. Cat. A.* 2004, 215, 81-87.
29. Chen, K.; Que, L., *J. Am. Chem. Soc.* 2001, 123, 6327-6337.
30. Chen, K.; Costas, M.; Kim, J. H.; Tipton, A. K.; Que, L., *J. Am. Chem. Soc.* 2002, 124, 3026-3035.